

Frequency-shifted laser feedback interferometry in non-planar ring oscillators

RONG ZHU,^{1,2,†} XUEZHEN GONG,^{1,†} WENXUN LI,¹ GHUOBIN ZHOU,¹
WEITONG FAN,¹ DANQING LIU,¹ CHUNZHAO MA,¹ JIE XU,¹ CHANGLEI
GUO,^{1,*} AND HSIEN-CHI YEH¹

¹MOE Key Laboratory of TianQin Mission, TianQin Research Center for Gravitational Physics & School of Physics and Astronomy, Frontiers Science Center for TianQin, CNSA Research Center for Gravitational Waves, Sun Yat-sen University (Zhuhai Campus), Zhuhai 519082, China

²Department of Physics, City University of Hong Kong, Tat Chee Avenue, Hong Kong SAR, China

[†]These authors contributed equally.

*guochlei@mail.sysu.edu.cn

Abstract: Laser feedback interferometry (LFI) has a wide range of applications such as displacement, distance and velocity measurements. LFI has been realized in many types of lasers but has never been reported in non-planar ring oscillators (NPRO) to the best of our knowledge. In this letter, we present a new type of LFI based on an NPRO laser. The intrinsic resistance to optical feedback in NPROs is broken under weak-magnetic-intensity condition, where stable bidirectional lasing is initiated in the ring cavity. The interference signal, i.e., the beat of the bidirectional lasing is with frequency from a few hundred of kilohertz to a few megahertz which is mainly determined by the applied magnetic intensity in NPRO. Frequency-shifted LFI is thus constructed in NPRO without using acousto-optic modulators as mostly used in conventional LFI. A theoretical model is established to well describe the phenomenon. In the end, micro-vibrational measurements are demonstrated to prove the potential application, where vibration-detection amplitude limit below 30 pm, vibration-detection frequency range from a few kilohertz to a few hundred kilohertz is achieved. Benefiting from the characteristics of tiny footprint, ruggedized structure, long lifetime and ultralow-noise of NPRO lasers, NPRO-based LFI may find important applications in industry, scientific research, military and aerospace.

1. Introduction

Laser feedback interferometry (LFI) has been widely used in metrology [1-6], laser parameters measurement [2], physical quantities measurement and other fields for its simple structure, easy alignment and high sensitivity [7-8]. It is based on self-mixing effect which uses reinjected photons back into the laser cavity to produce informative modulations of the laser intensity, frequency, phase or even polarization. Frequency-shifted LFI has been demonstrated to show better performance than heterodyne interferometry for a wide range of laser powers and detection noise levels [5-9]. This performance can be attributed to the amplification gain inside the laser cavity of the LFI, which is on the order of 10^3 to 10^6 in Class-B lasers [10-11]. In the meantime, the shifted frequency (near, resonant with, or much higher than the laser relaxation-oscillation frequency) gives a freedom to be tuned to find the best measurement resolution or sensitivity [9]. Accordingly, picometer displacement resolutions [12], sub-picowatt [13] or even single-photon sensitivities [14], have been demonstrated in solid-state microchip laser and fiber laser systems. However, because the roundtrip resonant frequencies are degenerate in most reciprocal laser resonators (i.e. Fabry-Perot or ring resonators without nonreciprocal elements), the required frequency shifts (from kilohertz to megahertz) have to rely on external devices, i.e., a pair of acousto-optic modulators (AOMs) [3-5,13-15]. This evidently adds complexity and cost to the system.

Nonplanar ring oscillators (NPROs) [16], with applied magnetic field, have non-degenerate resonant frequencies through nonreciprocal rotations of the polarizations in their clockwise and

counterclockwise roundtrips [17]. The resonant frequency differences from kilohertz to megahertz allow an NPRO to work as intrinsic frequency-shifted LFI without using AOMs. However, this phenomenon has never been reported before, to the best of our knowledge. The reason might be that the NPROs are in most cases working under high-intensity magnetic field (corresponding to high loss-differences), which makes them resistant to optical feedback [18]. Recently, we found that the loss-difference required for unidirectional lasing are not as large as a former empirical value of 0.01%, but could be as low as 0.0001% [19]. The lowered magnetic intensity decreases its resistance to optical feedback and leads to the observation of frequency-shifted LFI in NPROs.

In this letter, we demonstrate for the first time the frequency-shifted LFI in NPROs. Two-frequency rate equations [20] with the Lang - Kobayashi equation [21] are introduced to describe the feedback mechanism in NPRO. In the model, a same modulation term is seen in two stationary solutions which proves the theoretical validity of LFI in NPRO. This model gives a good explanation of the LFI measurement principle. In the end, LFI experiment is set up to demonstrate the application. The interference signals which come from the beat-notes of bidirectional lasing are measured and discussed. Moreover, vibration amplitudes from 30 pm to 550 pm at 100 kHz vibration frequency are detected with the NPRO LFI system. We believe our theory and experiment break a new path for frequency shifted LFI in NPROs.

2. Theory

Under weak magnetic intensity condition, the loss difference between the first two low-loss eigenmodes in NPRO is low so that the resistance to optical feedback is weakened [18]. The reinjected light from the CW/CCW (CW, clockwise, CCW, counter-clockwise) mode is coupled to the other mode. As a result, the bidirectional lasing in both CW and CCW direction are initiated in NPRO. Due to the mode coupling, the CW and CCW laser information is observed in each of the CW or CCW direction. This describes the basic physical phenomenon of LFI in NPRO. To theoretically explain this, we consider NPRO laser system (Nd:YAG with 808 nm pump laser and 1064 nm signal laser in our case) as a two-level system and suppose that each of the laser mode has corresponding population inversion, N_{CW} and N_{CCW} , which represent the population inversion of CW and CCW modes, respectively. Combined with Lang-Kobayashi equation [21], the complex forms of the two-frequency laser equations are given by:

$$\frac{d}{dt}E_{CW}(t)e^{i\omega_1 t} = \left[i\omega_{CW} + \frac{1}{2}(\varepsilon N_{CW} - \gamma_{CW}) \right] E_{CW}(t)e^{i\omega_1 t} \quad (1)$$

$$\frac{d}{dt}E_{CCW}(t)e^{i\omega_2 t} = \left[i\omega_{CCW} + \frac{1}{2}(\varepsilon N_{CCW} - \gamma_{CCW}) \right] E_{CCW}(t)e^{i\omega_2 t} + \gamma_{ext}E_{CW}(t - \tau)e^{i\omega_1(t-\tau)} \quad (2)$$

$$\frac{dN_{CW}}{dt} = \gamma[N_{01} - N_{CW}] - \varepsilon N_{CW} [|E_{CW}(t)|^2 + \xi_{12}|E_{CCW}(t)|^2] \quad (3)$$

$$\frac{dN_{CCW}}{dt} = \gamma[N_{02} - N_{CCW}] - \varepsilon N_{CCW} [|E_{CCW}(t)|^2 + \xi_{21}|E_{CW}(t)|^2] \quad (4)$$

Here, we consider the case when the reinjected light is CW. The laser cavity frequency of CW and CCW modes are ω_1 and ω_2 , respectively. E_{CW} and E_{CCW} represent the complex amplitude of the two electric fields, γ is the population inversion decay rate. γ_{CW} and γ_{CCW} are the decay rates of laser cavity in CW and CCW modes, which are assumed to be different because of the nonreciprocity of NPRO [17]. ε is the excited emission-coefficient which is related to the Einstein coefficient B . To describe the coupling between CW and CCW modes, coefficients ξ_{12} and ξ_{21} are introduced as the ratio of the cross- to the self-saturation coefficient, and $C = \xi_{12}\xi_{21}$ represents the nonlinear coupling constant [20]. N_{01} and N_{02} are the unsaturated population inversion of CW and CCW modes, respectively. γ_{ext} is reinjection rate of feedback

electric field which is related to the reflectivity of the target and coupling inside the cavity[10], and $\tau = 2D/c$ is the photon time delay between the laser and the target and D is the distance between them (for simplicity, the refractive index of the medium is 1).

In NPRO system, CW and CCW laser modes are from the same population inversion excitation. The whole lasing output power in two directions always be the same because of the conservation principle. We thus define the total unsaturated population inversion N_0 of NPRO as the sum of two directions, $N_0 = N_{01} + N_{02}$. It is seen as a constant under the same pumping condition and won't change by time and magnetic intensity. And we define $r_1 = N_{01}/N_{s1}$ and $r_2 = N_{02}/N_{s2}$ which are the corresponding excitation ratios for two modes [22], where $N_{s1} = \gamma_{CW}/\varepsilon$ and $N_{s2} = \gamma_{CCW}/\varepsilon$ are the stationary population inversions without optical feedback. Since the bidirectional laser modes share the total unsaturated population inversion N_0 , we consider the two excitation ratios are equal, which means $r_1 = r_2$. Then we get the relation between two unsaturated population inversions:

$$N_{01} = \frac{\gamma_{CW}}{\gamma_{CW} + \gamma_{CCW}} N_0 \quad (5)$$

$$N_{02} = \frac{\gamma_{CCW}}{\gamma_{CW} + \gamma_{CCW}} N_0 \quad (6)$$

We then define $\gamma_B = \gamma_{CW} + \gamma_{CCW}$ and I_{s1} and I_{s2} are the stationary optical intensities of the CW and CCW modes without optical feedback. After simplifying (1) - (4) without feedback term ($\gamma_{ext} = 0$) we have:

$$I_{s1} = |E_{CCW}(t)|^2 = \frac{\gamma(1 - \xi_{12})}{\varepsilon(1 - C)} \left(\frac{\varepsilon N_0}{\gamma_B} - 1 \right) \quad (7)$$

$$I_{s2} = |E_{CW}(t)|^2 = \frac{\gamma(1 - \xi_{21})}{\varepsilon(1 - C)} \left(\frac{\varepsilon N_0}{\gamma_B} - 1 \right) \quad (8)$$

With optical feedback, the stationary intensity solutions I_{s1}' and I_{s2}' are obtained from (1)-(4). For the interests of simplicity, we consider the case of the slowly varying amplitude and the photon time delay τ is much shorter than the period of the beat signal between the two modes, which implies $E(t - \tau) \approx E(t)$. Then we have:

$$\begin{aligned} I_{s1}' &= \frac{\gamma(1 - \xi_{12})}{\varepsilon(1 - C)} \left(\frac{\varepsilon N_0}{(\gamma_{CW} + \gamma_{CCW}) - 2\gamma_{ext} \cos(\Delta\omega t - \omega_1\tau)} - 1 \right) \\ &\approx I_{s1} \left(1 + \frac{r}{r-1} \frac{\gamma_{ext}}{\gamma_B} \cos(\Delta\omega t - \omega_1\tau) \right) \end{aligned} \quad (9)$$

$$\begin{aligned} I_{s2}' &= \frac{\gamma(1 - \xi_{21})}{\varepsilon(1 - C)} \left(\frac{\varepsilon N_0}{(\gamma_{CW} + \gamma_{CCW}) - 2\gamma_{ext} \cos(\Delta\omega t - \omega_1\tau)} - 1 \right) \\ &\approx I_{s2} \left(1 + \frac{r}{r-1} \frac{\gamma_{ext}}{\gamma_B} \cos(\Delta\omega t - \omega_1\tau) \right) \end{aligned} \quad (10)$$

where $\Delta\omega = \omega_2 - \omega_1$ and we consider the case when $\gamma_{ext}\tau \ll 1$. From (9)-(10) we can see that after introducing the external optical feedback term to the laser equations, the intensity solutions become the steady-state intensity solutions without optical feedback (7)-(8) plus a modulation term with target signal, and this modulation term shows up in both solutions. These equations prove that the NPRO feedback system can achieve self-feedback interferometry with a target signal acting as the amplitude modulation.

3. Experiment

To verify the theoretical predictions of the LFI in NPRO, we build an experiment as shown schematically in Fig.1. Laser diode operating at 808 nm wavelength is the pumping source for NPRO, where Nd:YAG crystal is the gain material. A lens ($f = 15$ mm) is used to focus the pump light onto the NPRO. The NPRO has a dimension of $3\text{ mm} \times 8\text{ mm} \times 12\text{ mm}$ and exhibits an incident angle of 30° , an out-of-plane angle of 90° . The front surface of the crystal is coated with high-transmittance at 808 nm and high-reflectance (99.8% for *S* polarization and 94% for *P* polarization) at 1064 nm. The NPRO operates under a temperature of around 25°C with active temperature controller. The distance d between the permanent magnet and the NPRO is controlled by a one-dimensional transition-stage. In this way, the magnetic intensity applied on the NPRO can be tuned with d . The direction of magnetic field is chosen for CW emission under unidirectional condition. More details on the experimental parameters are described in [19] and [22]. A dichroic mirror is placed between the laser diode and the NPRO, with high transmittance at 808 nm and high reflectance at 1064 nm. This mirror will reflect the CW laser towards an external target and simultaneously collect the feedback signal from the target to the NPRO. Between the target and the dichroic mirror, a polarization beam splitter is used to split part of the light for interference measurements, where the light is attenuated before detection. A low-noise photodetector with transimpedance amplifier (Thorlabs, PDA05CF2) is used here, and the electronic signal is processed by an electronic spectrum analyzer (Rohde & Schwarz, FSV3007). On the CCW light path, a similar measurement (shadow zone in Fig. 1) can also be constructed. We found the measurement sensitivity between the two paths is slightly different, which will be investigated in future study. In the next, the measurements are taken on the CW light path.

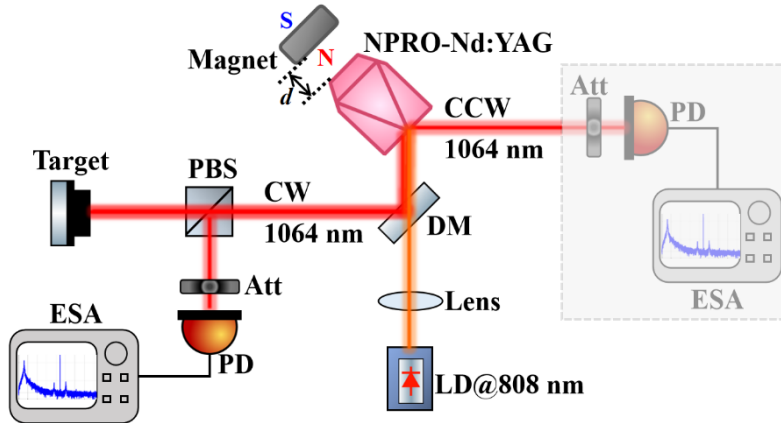


Fig. 1. Schematic of the experimental setup for the NPRO LFI system. d is the distance between the magnet and the NPRO. N and S represent the magnetic poles. LD, laser diode; DM, dichroic mirror with high transmittance at 808 nm and high reflection at 1064 nm; CW, clockwise; CCW, counter-clockwise; PBS, polarization beam splitter; Att, optical attenuator; PD, photodetector; ESA, electronic spectrum analyzer. The shadow zone on the CCW light path can realize similar measurements as that on the CW and is not used in this study.

A high-reflection ($>99.5\%$ @1064 nm) mirror is firstly used as the target, whose position is finely adjusted to find the strongest beat signal. The mirror is decimeters far away from the NPRO and the CW and CCW light powers are as high as tens of milliwatt (under a pump power of 400 mW at 808 nm). A typical beat signal measured by the electronic spectrum analyzer is shown by the relative amplitude density in Fig. 2(a), where the resolution bandwidth (RBW) is 500 Hz. The beat signal is with a center frequency of 883 kHz. The two sidebands around it as well as the strong noise peak at around 123 kHz are from the relaxation oscillations of the NPRO laser itself. From Fig. 2(a) one can see the beat signal has a good signal-to-noise ratio. Further frequency stability measurement using a frequency counter shows that the frequency

noise of the beat signal is as low as $10 \text{ Hz/Hz}^{1/2}$ with Fourier frequency higher than 5 Hz (not shown here), which is a good indication for precision measurement applications. Fig. 2(b) shows the beat frequency versus magnet distance d . By scanning d from 1 mm to 9 mm one finds that the beat-note frequency is decreased from $\sim 1.3 \text{ MHz}$ to $\sim 460 \text{ kHz}$. We have tested a few NPRO samples and found the beat frequencies are mostly stable in the range of hundreds of kilohertz to over one megahertz. The lowest frequency can go to the low frequency side of the relaxation oscillation. Keeping increasing the distance will lead the competition between the two laser modes and the beat signal becomes unstable [19] or even disappears.

In conventional LFI, when the feedback power ratio is higher than a certain value (typically -30 dB or lower), chaos may emerge in the LFI system [2], which significantly deteriorates the applications. We found this does not happen in our NPRO LFI system. We estimated the feedback power ratio which is more than -10 dB (10%) by measuring the optical power on both the CW and CCW paths, before and after the LFI is built. This indicates a significant difference between the NPRO LFI and other LFI systems. We further calculated the feedback level C [2] by substituting parameters of our system (where the linewidth enhancement factor α is 1 for Nd:YAG crystal), which gives a value of ~ 0.1 . The NPRO LFI characterization with different feedback power ratios and C values will be studied in the future.

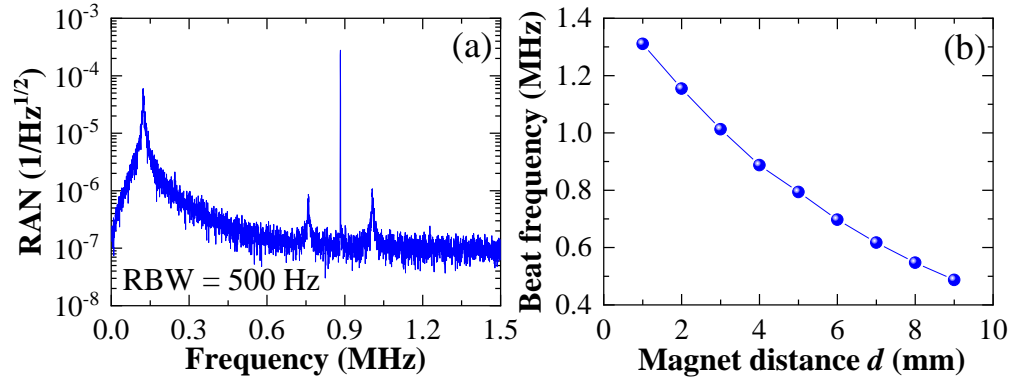


Fig. 2. (a) Electronic spectrum measured as relative amplitude noise (RAN) of a typical beat signal (centered at 882.7 kHz) with the laser relaxation-oscillation noises (fundamental frequency centered at 122.6 kHz). The RBW is 500 Hz. (b) Experimentally measured beat frequency versus magnet distance d .

To demonstrate the application, we then replace the target with a piezo-mirror, where the mirror adhesive to a single-layer piezoelectric ceramic can simulate a micro-vibration up to hundreds of kilohertz. The piezo is driven by a sine-wave voltage from a function generator. The oscillating mirror will simultaneously change the optical path length between the target and the NPRO. Finally, this change is detected by the photodetector and processed by the electronic spectrum analyzer as reflected in equations (9) and (10). Figure 3(a) shows typical electronic spectra when the 100 kHz sine-wave voltage modulation is applied on the piezo, where the corresponding piezo driving V_{pp} (peak to peak value) are respective 0.4 V, 0.8 V, 1.6 V and 3.2 V, and the RBW is 2 kHz. The two thin sidebands symmetrically distribute around the beat signal (at 933 kHz) with a 100 kHz frequency difference, which proves that the sine-wave modulation induced micro-vibration has been detected by the NPRO LFI system. The height of the modulation sideband reflects the amplitude of the target vibration. The driving voltage amplitude is tuned from 200 mV to 4.1 V, and the corresponding electronic spectra are collected. In order to resolve the vibration amplitude, a demodulation method from [23] is adopted, where the vibration amplitude A_v is related to the ratio of the sideband power P_s and beat signal power P_b as:

$$A_v = \frac{\lambda P_s}{2\pi P_b} \quad (11)$$

Here, λ is the laser wavelength of 1064 nm. Finally, the vibration amplitude A_v versus the applied voltage V_{pp} are resolved as shown in Fig. 3(b), where 30 pm to 550 pm vibration amplitudes are detected at 100 kHz. Linear fitting gives a goodness of $R^2 = 0.9993$, which means this detection is working in a very good linear range. Note these performances are comparable to that shown in [13], where AOMs are used to shift the beat frequency.

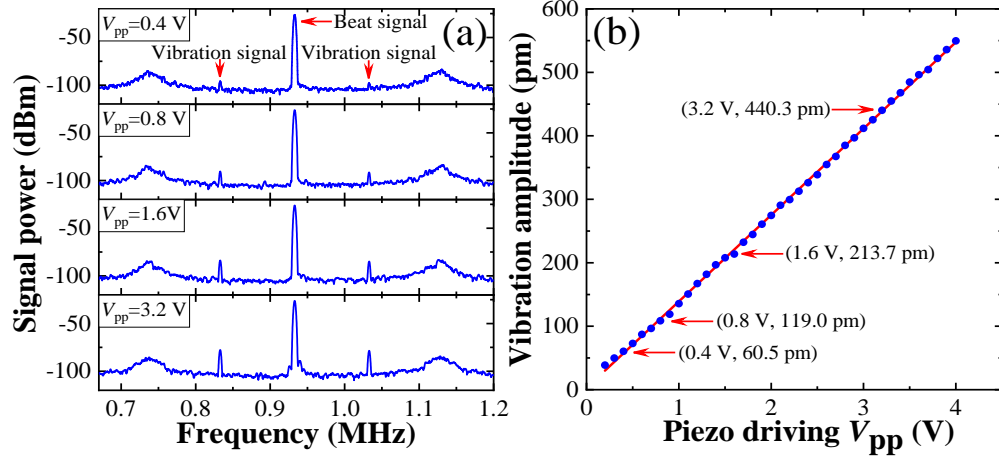


Fig. 3. (a) Electronic spectra (measured as signal power) of the vibration detection with the beat signal (centered at 933 kHz), the vibration signals (two thin sidebands) and the laser relaxation-oscillation noises (two broad sidebands). The corresponding piezo driving V_{pp} of 0.4 V, 0.8 V, 1.6 V and 3.2 V are shown, respectively. The RBW is 2 kHz. (b) Resolved vibration amplitude versus piezo driving voltage amplitude V_{pp} . The vibration frequency is at 100 kHz. Blue dots are from experimental measurements, red line is linear fit. The goodness of the linear fit is 0.9993.

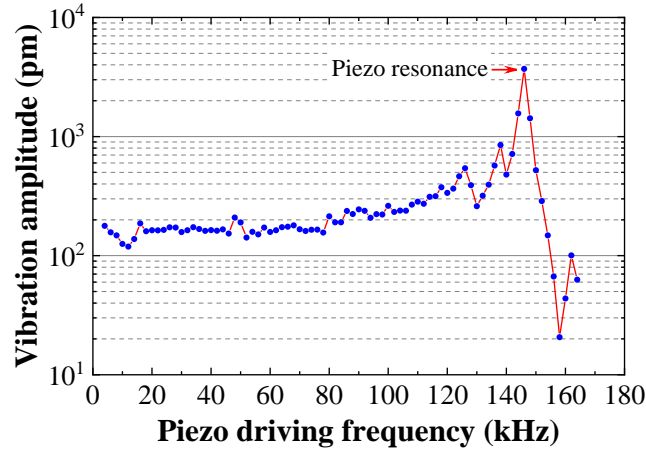


Fig. 4. Vibration amplitude versus piezo driving frequency at constant piezo driving V_{pp} . The resonance peak at around 146 kHz is from the piezo itself.

In Fig. 3(b), the first point (0.2 V, 30.0 pm) deviates the fitting line. This means the minimum vibration detection is nearly reached, which is determined by P_s/P_b as indicated by formula (11). Further extending the limit needs increasing the signal-to-noise-ratio of the beat signal. In order to give the vibration frequency measurement range, we have scanned the piezo driving frequency with constant V_{pp} and calculated the corresponding vibration amplitude A_v . The

typical results are shown in Fig. 4. One can see that the lowest detected vibration frequency is about 2 kHz, which is mainly limited by the beat signal linewidth at present. It can be further shrunk by beat frequency stabilization in the future. This, in turn, may also extend the minimum vibration amplitude detection limit. The upper bound of the vibration detection frequency is limited by the piezo itself used in the experiment. We have briefly increased the driving frequency to more than 500 kHz, the vibration signals can still be seen. Note there is a resonance peak at around 146 kHz in Fig.4, which is from the piezo itself.

We then analyze the accuracy of our vibration detection theoretically due to the limit of calibration tool. We first use the method shown in [23] to calculate the vibration amplitude under the first-order approximate solution, and find the inaccuracy is below 1% when the vibration amplitude is below 24 nm. We then build a three-dimensional finite-element model with piezo and mirror to simulate the vibration amplitude under experimental parameters. We find the calculated vibration amplitude is on the same order-of-magnitude as the measurements. Thus, the measurement accuracy is indirectly verified. Note the accuracy can also be affected by the optical path length instability induced by environment such as temperature, vibration and airflow. However, these factors are mostly influencing the detection in the low frequency range (below 1 kHz), and thus are not considered in this experiment.

4. Conclusions

In summary, we present a new type of laser feedback interferometry based on an NPRO laser system. Under weak magnetic intensity, the reinjected light drives an NPRO works in stable bidirectional lasing regime which constructs naturally a frequency-shifted LFI system. A theoretical model based on two-frequency rate equations and Lang–Kobayashi equation is built to explain the LFI measurement principle. The beat frequency shift with magnet position is experimentally studied. Moreover, vibration detection is demonstrated to prove the potential application, where the vibration-detection amplitude limit is below 30 pm, the vibration-detection frequency range is from a few kilohertz to a few hundred kilohertz. The vibration detection frequency range, minimum amplitude limit and amplitude accuracy are further discussed. Benefiting from its tiny footprint, rigid structure and excellent detection resolution and accuracy, the NPRO-based frequency-shifted LFI system may find important applications in vibration, velocimetry, displacement and rotation measurements with high sensitivities.

Funding. National Natural Science Foundation of China (12404489); Fundamental Research Funds for the Central Universities, Sun Yat-sen University (24QNPY162). National Key Research and Development Program of China (2020YFC2200200); Major Projects of Basic and Applied Basic Research in Guangdong Province (2019B030302001).

Acknowledgments. The authors would like to thank Huizong Duan for helpful discussions.

Disclosures. The authors declare no conflicts of interest.

Data availability. Data underlying the results presented in this paper are not publicly available at this time but may be obtained from the authors upon reasonable request.

References

1. S. Zhang, S. Zhang, Y. Tan, and L. Sun, "A microchip laser source with stable intensity and frequency used for self-mixing interferometry," *Rev. Sci. Instrum.* **87**(5), 113-119 (2016).
2. T. Taimre, M. Nikolic, K. Bertling, Y. L. Lim, T. Bosch, and A. D. Rakic, "Laser feedback interferometry: a tutorial on the self-mixing effect for coherent sensing," *Adv. Opt. Photonics* **7**, 570-631 (2015).
3. C. Xu, S. Zhang, Y. Tan, and S. Zhao, "Inner structure detection by optical tomography technology based on feedback of microchip Nd:YAG lasers," *Opt. Express* **21**(10), 11819-11826 (2013).
4. J. Li, H. Niu, and Y. Niu, "Laser feedback interferometry and applications: a review," *Opt. Engineering* **56**(5), 050901-050901 (2017).

5. E. Lacot, O. Jacquin, G. Roussely, O. Hugon, and H. Guillet de Chatellus, "Comparative study of autodyne and heterodyne laser interferometry for imaging," *J. Opt. Soc. Am. A* **27**(11), 2450-2458 (2010).
6. S. Donati, "Developing self-mixing interferometry for instrumentation and measurements," *Laser Photonics Rev.* **6**(3), 393-417 (2012).
7. S. Okamoto, H. Takeda, and F. Kannari, "Ultrahighly sensitive laser Doppler velocity meter with a diode-pumped Nd:YVO₄ microchip laser," *Rev. Sci. Instrum.* **66**, 3116-3120 (1995).
8. R. Kawai, Y. Asakawa, and K. Otsuka, "Ultrahigh-sensitivity selfmixing laser Doppler velocimetry with laser-diode-pumped microchip LiNdP₄O₁₂ lasers," *IEEE Photon. Technol. Lett.* **11**, 706-708 (1999).
9. O. Jacquin, E. Lacot, W. Glastre, O. Hugon, and H. Guillet de Chatellus, "Experimental comparison of autodyne and heterodyne laser interferometry using an Nd:YVO₄ microchip laser," *J. Opt. Soc. Am. A* **28**(8), 1741-1746 (2011).
10. E. Lacot, R. Day, F. Stoeckel, "Coherent laser detection by frequency-shifted optical feedback," *Phys. Rev. A* **64**, 043815 (2001).
11. K. Otsuka, "Effects of external perturbations on LiNdP₄O₁₂ lasers," *IEEE J. Quantum Electron.* **15**(7), 655-663 (1979).
12. Y. Zhao, D. Zhu, Y. Chen, Y. Tu, L. Lu, "All-fiber self-mixing laser Doppler velocimetry with much less than 0.1pW optical feedback based on adjustable gain," *Opt. Lett.* **45**(13), 3565-3568 (2020).
13. D. Zhu, Y. Zhao, Y. Tu, H. Li, L. Xu, B. Yu, and L. Lu, "All-fiber laser feedback interferometer using a DBR fiber laser for effective sub-picometer displacement measurement," *Opt. Lett.* **46**(1), 114-117 (2021).
14. Z. Xu, J. Li, S. Zhang, Y. Tan, X. Zhang, X. Lin, X. Wan, and S. Zhuang, "Remote eavesdropping at 200 meters distance based on laser feedback interferometry with single-photon sensitivity," *Opt. Lasers Eng.* **141**(1), 106562 (2021).
15. E. Lacot, O. Hugon, "Frequency-shifted optical feedback in a pumping laser diode dynamically amplified by a microchip laser," *Appl. Opt.* **43**(25), 4915-4921 (2004).
16. T.J. Kane, R.L. Byer. "Monolithic unidirectional single-mode Nd:YAG ring laser," *Opt. Lett.* **10**(2), 65-67 (1985).
17. A. C. Nilsson, E. K. Gustafson, and R. L. Byer, "Eigenpolarization theory of monolithic nonplanar ring oscillators," *IEEE J. Quantum Electron* **25**(4), 767-790 (1989).
18. A. C. Nilsson, T. J. Kane, and R. L. Byer, "Monolithic nonplanar ring lasers - Resistance to optical feedback," *Proc. SPIE* **912**, 13-18 (1988).
19. G. Zhou, R. Zhu, C. Ma, X. Gong, W. Fan, S. Zhou, J. Xu, C. Guo, and Hsien-Chi Yeh, "Unidirectional operation criterion in monolithic nonplanar ring oscillators," *Opt. Lett.* **48**(11), 3047-3050 (2023).
20. De, Pal, E. Amili, G. Pillet, G. Baili, M. Alouini, I. Sagnes, R. Ghosh, and F. Bretenaker, "Intensity noise correlations in a two-frequency VECSEL," *Opt. Express* **21**(3), 2538-2550 (2013).
21. L. Roy, K. Kobayashi. "External optical feedback effects on semiconductor injection laser properties," *IEEE J. Quantum Electron.* **16**(3), 347-355 (1980).
22. W. Fan, C. Ma, D. Liu, R. Zhu, G. Zhou, X. Gong, S. Zhou, J. Xu, W. Yuan, C. Guo, and Hsien-Chi Yeh, "Dual-frequency fundamental-mode NPRO laser for low-noise microwave generation," *Opt. Express* **31**(8), 13402-13413 (2023).
23. H. Martinussen, A. Aksnes, and H. E. Engan, "Wide frequency range measurements of absolute phase and amplitude of vibrations in micro- and nanostructures by optical interferometry," *Opt. Express* **15**(18), 11370-11384 (2007).